4. A FEW EXAMPLES OF ION OR ELECTRON MOTION

4.1 Field-free section

Let us consider a straight section with enlarged vacuum chamber (Fig. 11). The potential well at the centre of the beam is

$$V_0 = \frac{\lambda}{2\pi\varepsilon_0}\left\{\ln\left(\frac{r_0}{a}\right)+\frac{1}{2}\right\} \qquad (39)$$

giving the curve of potential represented in Fig. 11 as a function of the azimuth. In this example the ions created between B and C will be trapped, the ions created between A and B will drift towards C and continue to the right with an energy between 0 and 6 eV.

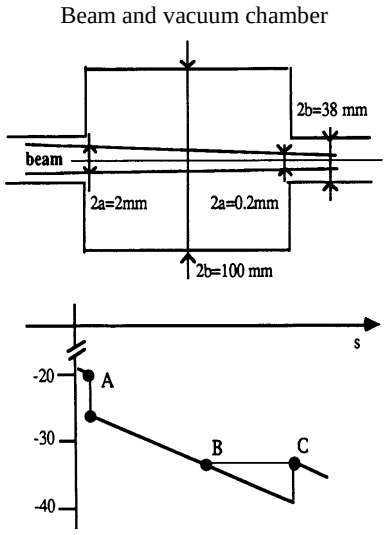

Fig. 11 Potential well in a field-free section.

4.2 Pure dipole field

With our nominal beam parameters (section 1), the electric field at the edge of the beam is 1.2×10^4 Vm^{-1} so that the cross-field drift velocity varies from zero at the centre to 8.6×10^3 ms^{-1} at the edge of the beam. The corresponding energies are 2×10^{-4} eV for electrons and 11 eV for N_2^+ ions. The cyclotron radius for electrons in the centre with energy of about 1 eV is 2.4 μm (0.6 mm for ions).

Particles with the same charge as the beam are chased out of the potential well in the vertical plane. Particles with opposite charge drift towards the end of the magnet, but are contained in the potential well in the vertical plane.

4.3 Combined function magnet

Let us consider a magnet like the EPA magnet with a field of 1.4 T on the central orbit and a gradient of 1 T/m on the central orbit. We have seen that the typical energy of particles created in the potential well is a few electron volts, the corresponding velocities are (section 3.1):

for ions ~ 2.6×10^3 ms^{-1}.

for electrons ~ 6×10^5 ms^{-1}.

The cyclotron radii in the centre are very small. The additional gradient drift for ions or electrons of 1 eV is of the order of 0.5 ms^{-1} and therefore negligible with respect to the cross-field drift.

4.4 The quadrupole field

If the beam is centred in a quadrupole with gradient 3 Tm^{-1}, the cross-field drift at equilibrium at the edge of the beam will be Eq. (37)

$$\upsilon_c = 8 \times 10^6 \text{ m s}^{-1}$$

corresponding to an energy for ions of 9 MeV. This energy would have to be provided by the potential well, which is of only a few tens of volts, so that the equilibrium required for the cross-field drift will never be reached. The electric field of the potential well dominates the ion motion.

Particles with the same charge as the circulating beam are chased toward the poles of the quadrupole. In some cases a magnetic mirror effect could ensure the containment of these particles.

4.5 Undulator

The field of an undulator is dipolar but with alternatively positive and negative polarity along the azimuth. The main effect in the horizontal plane is the cross-field drift, but the fact that the field is alternated gives a possibility of containment. In the vertical plane the field is concentrated in the poles so that a magnetic mirror effect can develop. This mechanism can be effective for electrons or ions depending on the geometry and the beam polarity. Since the potential well is not required to achieve containment, it is not easy to find the mechanism which limits the accumulation of ions in an undulator.

5. BUNCHED BEAMS

All previous studies are in principle valid only for unbunched circulating beams. In fact the bunching only introduces additional effects. In Refs. [7, 14, 57, 75], one finds a study of the stability of ions in single-beam and colliding-beam machines. We shall only summarise the results of this study in the case of single-beam machines.

Here, we have changed the definition of the neutralisation factor η from the local definition used in Ref. [14] to the average definition given above in Eq. (1). This explains the difference between our formulae and those of Ref. [14].

At a given azimuth, an ion sees successively the focusing (or defocusing) forces induced by the bunch passage, followed by a drift time between bunches. If a vertical dipole magnetic field is applied, the horizontal transverse and longitudinal motions will be coupled, the vertical motion however being independent of the magnetic field. The horizontal motion will not be studied here [83]. It gives similar results in drift space; in a bending magnet the horizontal motion is usually stable. The present study is therefore limited to the vertical motion.

The forces induced by the passage of a bunch have been studied by several authors (e.g. [8, 14]). With the time as independent variable the bunch passage is similar to a focusing (or defocusing) lens; if the bunch is short the effect on the ion can be described by a matrix equivalent to a thin lens. The non-linear effects are not considered here.

Let y and $dy = \dot{y}$ be the position and speed of the ion. Then the passage of a bunch is described by

$$\begin{pmatrix} y \\ \dot{y} \end{pmatrix}_1 = \begin{pmatrix} 1 & 0 \\ \alpha & 1 \end{pmatrix} \begin{pmatrix} y \\ \dot{y} \end{pmatrix}_0$$

with

$$\alpha = \frac{n_e}{n} \frac{4 r_p}{\beta b (a+b)} \frac{1}{A} \tag{40}$$

where n_e/n *is* the charge per bunch, n the number of bunches, r_p the classical proton radius, a, b the beam size, horizontal resp. vertical, A the atomic weight of the ion and βc the velocity of the circulating beam.

Between bunches the ion drifts freely during the time $t = T/n$. Where T is the revolution time, corresponding to the matrix transformation

$$\begin{pmatrix} 1 & t \\ 0 & 1 \end{pmatrix}.$$

One period of the forces applied is described by the matrix product

$$M = \begin{pmatrix} 1 & t \\ 0 & 1 \end{pmatrix} \begin{pmatrix} 1 & 0 \\ \alpha & 1 \end{pmatrix}$$

The stability is insured if the trace of the matrix satisfies

$$-2 < Tr(M) < +2$$

that is for

$$-1 < \left(1 \pm \alpha \frac{T}{2n}\right) < +1 .$$

The + sign is to be selected for cases where the beam and the ion are of the same sign. Electron beams therefore cannot accumulate electrons, and proton beams cannot accumulate positive ions, which is obvious. For the opposite sign, the requirement is:

$$1 - \alpha \frac{T}{2n} > -1 .$$

If $A.m_p$ is the mass of the ion, one can express the above formulae by the following criterion: all ionic masses larger than a critical mass A_c will be accumulated.

$$A_c = \frac{n_e}{n} \frac{r_p}{n} \frac{2\pi R}{\beta \cdot b^2 \left(1 + \frac{a}{b}\right)} . \qquad (41)$$

In most practical cases the critical mass varies between 0.1 and 100. This explains why electrons ($A \simeq 1/2000$) never accumulate in bunched beams of positrons or protons.

In bunched beams of electrons with a large number of bunches (e.g. synchrotron radiation sources) the critical mass can be very small ~ 10^{-2}. Then the ion accumulation can be treated as in DC beams: the ions are too heavy to 'see' that the beam is bunched.

When the critical mass is above 44, the ions usually found in vacuum systems cannot accumulate.

Intermediate cases:

$$1 < A_c < 44$$

require a detailed analysis [14].

Note:

There is some confusion on the values to be used for *a* and *b* after a real measurement of particle distributions. They are related to the central density of the transverse distribution of particles. If the measured distributions were rectangular then *a* and *b* would be the measure of the real half width of the distributions. If the distributions are Gaussian, a simple calculation shows that

$$a = \sigma_x \sqrt{2}$$

$$b = \sigma_y \sqrt{2}$$

6. CLEARING MEANS

6.1 Missing bunches (electron storage rings)

Many small electron storage rings prone to ion trapping have partly solved their problem by introducing one or several gaps in the bunch train by not filling certain buckets at injection. Over one revolution period of a train of *p* consecutive bunches, the motion (here vertical) of a trapped ion is the solution of:

$$\begin{bmatrix} y \\ \dot{y} \end{bmatrix}_1 = M \begin{bmatrix} y \\ \dot{y} \end{bmatrix}_0$$

with the transfer matrix

$$M = \left(\begin{bmatrix} 1 & 0 \\ \alpha & 1 \end{bmatrix} \begin{bmatrix} 1 & t \\ 0 & 1 \end{bmatrix} \right)^p \begin{bmatrix} 1 & (h-p)t \\ 0 & 1 \end{bmatrix} \tag{42}$$

where the terms in parenthesis represent the linear kick received at the p bunch passages interleaved with drifts of duration t, f being the radiofrequency. The period of p successive kicks plus drifts is terminated by the drift in the time interval $(h\text{-}p)\ t$, where h is the cavity harmonic, i.e. the maximum number of bunches that the machine can handle. The Floquet's condition of stability for the ion of mass-to-charge A:

$$-2 < Tr\,(M) < 2$$

does not lead to a simple criterium defining which A's are stable. Rather, the trace of the transfer matrix (42) is of order p in N, the total number of circulating particles. This means that there are p stable bands of ion mass-to-charge ratios for a given N, or that a given ion will be stable or unstable, depending on the number of beam particles. Figure 12 illustrates the conditions of linear stability for various ions in the EPA ring, as a function of the number of beam particles and consecutive bunches [89].

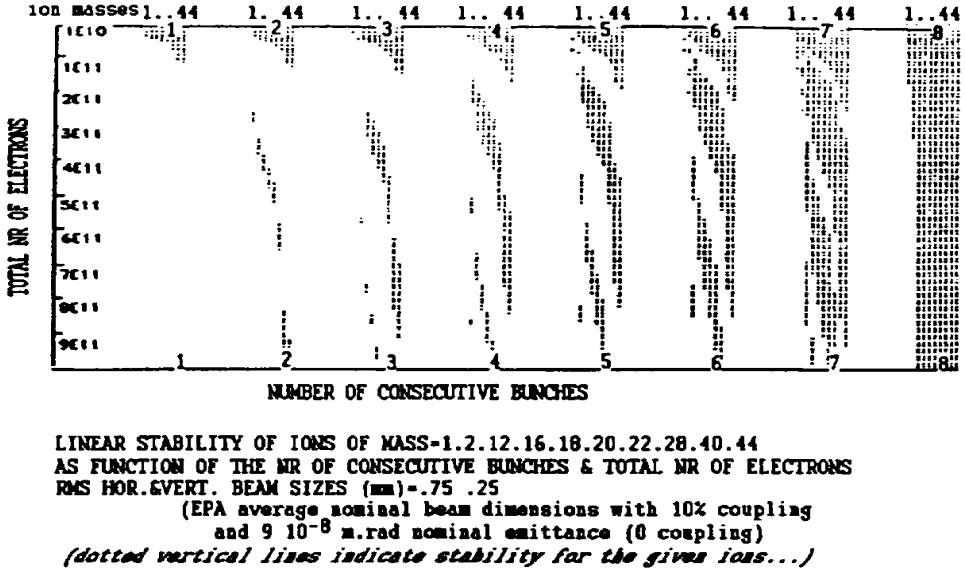

Fig. 12 Linear stability of ions in EPA as a function of total beam intensity and number of consecutive bunches for nominal beam emittances.

Although not always absent, ion trapping is indeed less severe with missing bunches. This stems from the fact that since a given trapped ion can be further ionised, it then has a good chance of falling in an unstable band and thus of being cleared.

6.2 Clearing electrodes

Clearing electrodes consisting of negatively polarised plates fitted into the vacuum chamber provide a transverse electric field, which diverts beam-channelled ions onto them, where they are neutralised and return into the gas phase. Figure 13 qualitatively represents the potential variation across a vacuum chamber of radius r_c, with an electrode on one side with a potential of U_{ce}.

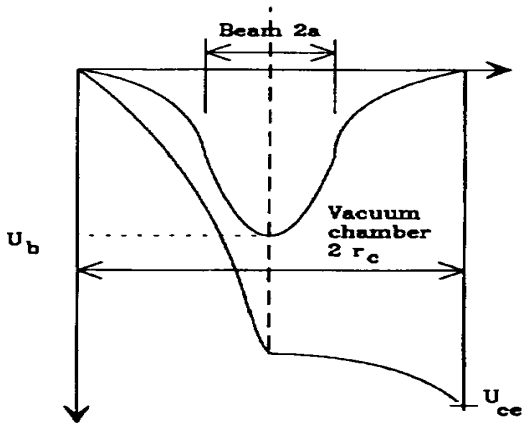

Fig. 13 Transverse potential distribution across a vacuum chamber due to the beam space charge and a clearing electrode.

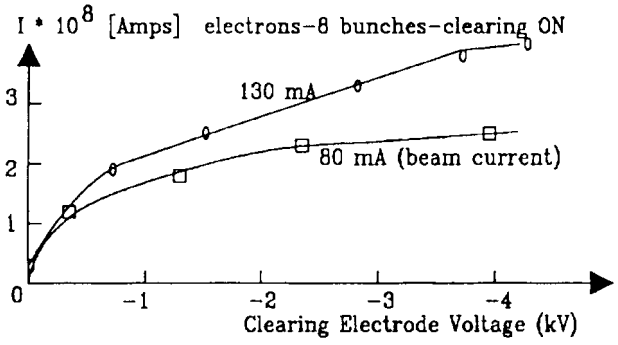

Fig. 14 Extracted ion current vs. electrode voltage in EPA.

A minimum condition for capture of the passing ion is that the transverse field provided by the electrode equals the maximum beam space charge field:

$$\frac{U_{ce}}{2r_c} > E(a) \sim \frac{I}{2\pi\beta c\varepsilon_0 a} \tag{43}$$

In fact, because ions may have — as we have seen — transverse and longitudinal velocities corresponding to energies of up to a few eV (possibly up to the field at the centre if singly ionised) and because a clearing electrode is necessarily limited in size, the field provided by the electrode must usually be larger than the calculated beam field. For instance in the EPA ring, where electrodes are of the button type with a diameter of 20 mm and installed flush to the beam, transverse clearing in field-free regions is complete with the following parameters [89]:

$$U_{ce} = 6 \text{ kV}$$

electrode field: 30 kV/m on beam axis. Beam max. field: 12 kV/m for I = 0.3 A and ~ 10^{-8} m-rad horizontal emittance with 10% coupling.

Measurement of the electrode clearing current as a function of the applied voltage provides a verification of the required maximum to be applied for full clearing, since the current will saturate once a sufficient field is reached (Fig. 14). The number and the optimum location of electrodes are in principle dictated by the tolerable degree of residual neutralisation. In practice, even with a large number of electrodes, uncleared pockets always remain and contribute to typical residual neutralisations of a fraction to a few percent.

Few (if any) small electron storage rings exist which have reached a fully satisfactory ion-free situation, even with clearing electrodes. Perhaps one reason for this is that clearing systems have not been up to now very complete, partly owing to the fact that clearing electrodes complicate the mechanical design of the vacuum chamber and may contribute to the machine impedance. At CERN (EPA), button-type clearing electrodes presenting negligible coupling characteristics to the beam have been designed. They are made of a ceramic body, coated with a highly resistive glass layer (thick-film hybrid technology), and are terminated with a highly lossy wide-band filter as shown in Fig. 15.

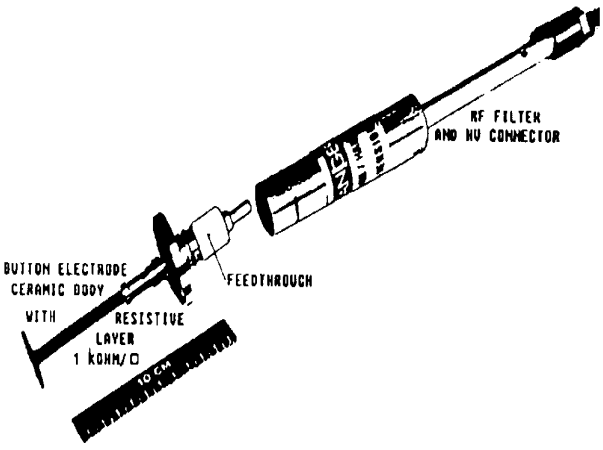

Fig. 15 EPA button-type clearing electrode.

6.3 Resonant transverse shaking of the beam

Neutralisation effects can be reduced when exciting vertical coherent oscillations with a transverse kicker at a given frequency [103], both in electron storage rings (bunched) and antiproton accumulators (unbunched). This technique of “RF knock out” of neutralising ions has been nicknamed “beam shaking”. It has been determinant in solving ion problems in the CERN AA, where it has been studied both theoretically [103] and experimentally [102] and where it was permanently implemented, with the following parameters:

shaking: vertical
shaking frequency: 490 kHz
sideband frequency (fractional tune q_v):480 kHz
length of kicker electrodes: 0.6 m
kicker field: ~ 20 V/cm

Beam shaking experimental observations can be summarised as follows:

1) Beam shaking works best when applied vertically: one possible reason is that neutralisation is high in dipole fields (low ion drift velocity) where the motion along the lines of force is the only practical degree of freedom.

2) To work, beam shaking relies on the longitudinal motion of the ions. Due to changing beam dimensions, the ion "plasma frequency" spectrum is wide compared to the "knock out” frequency: ions have to "sweep" through this resonance. For this, they must be free to move longitudinally.

3) Beam shaking depends on the non-linearity of the beam space-charge field: this allows the “lock on” of the sweeping ions onto the resonance where they keep large oscillation amplitudes, thus reducing their density in the beam centre.

4) Beam shaking is efficient even with RF kicker fields of only a few 10 V/cm, provided it is applied close to a beam betatron side band whose frequency lies close to the ion plasma frequency. In this case, the beam resonant response ensures sufficiently large non-linear forces on the ion. Experimentally, it is found that for a weakly exciting RF field, shaking works best above a band (n+Q) or below a band (n-Q). This observation of asymmetry of weak resonant shaking is important in that it validates the non-linear character of the ion motion and the “lock on" conditions.

To illustrate this in a simple way, we use a quasi-linear description of the two-body resonant condition [117] for an unbunched beam. We consider only one ion species i, of mass-to-charge ratio A_i, with the following definitions:

Ω: circular revolution frequency of circulating beam ($\Omega = 2\pi f_i$)

$Q_i = 2\pi f_i/\Omega$: the ion bounce number in the beam potential well

$$\Omega_i^{\,2} Q_i^2 = \frac{2N_p r_p c^2}{\pi b(a+b)\gamma R} \ .$$

If Q_v, is the beam particle unperturbed incoherent tune and Q_p the beam particle bounce number in the ion-potential well where

$$\Omega^2 Q_p^2 = \frac{2N_i r_p c^2}{\pi b(a+b)\gamma R}$$

and

$$Q = \left(Q_v^2 + Q_p^2\right)^{1/2}$$

is the perturbed beam tune, then a beam particle and an ion obey the coupled set of linear differential equations

particle: $$\left(\frac{\partial^2}{\partial t^2} + \Omega\frac{\partial^2}{\partial\theta^2}\right)y_p + Q^2\Omega^2 y_p - Q_p{}^2\Omega^2\bar{y}_i = Fe^{i\omega t} \tag{44}$$

ion: $$\left(\frac{d^2}{dt^2}\right)y_i + \Omega_i{}^2\Omega^2\left(y_i - \bar{y}_p\right) = 0$$

where the bar on y denotes the average vertical position of each beam and the $Fe^{i\omega t}$ term is the harmonic of the external driving force close to beam ion resonance:

$$\omega_f \; (n \pm Q)\Omega_f \; Q_i\,\Omega \;\; .$$

Assuming solutions of the form:

$$y_p = \xi_p e^{i(n\theta+\omega t)}$$

$$y_i = \xi_i e^{i\omega t}$$

the ion amplitude becomes:

$$y_i = \frac{Q_i^2\,\frac{F}{\Omega^2}\,e^{i\omega t}}{\left(x^2 - Q_i^2\right)\left((n+x)^2 - Q^2\right) - Q_p^2 Q_i^2} \tag{45}$$

with $$x = \frac{\omega}{\Omega} \rightarrow (n \pm Q) \sim Q_i \;\; .$$

Therefore, shaking works when y_i becomes large, i.e. when the denominator in Eq. (45) $\rightarrow 0$. But, as shown in Fig. 16, as the ions gain large amplitude, we have non-linear detuning such that $x^2 > Q_i^2$ (lock on). Therefore for y_i to become large, requires that:

$$(n+x)^2 - Q^2 > 0$$

i.e.: $x < n - Q$ for excitation near a "slow-wave" beam frequency: $\omega \cong (n-Q)\Omega; n > Q$

$x > n + Q$ for a "fast-wave" frequency : $\omega \cong (n+Q)\Omega; n > Q$.

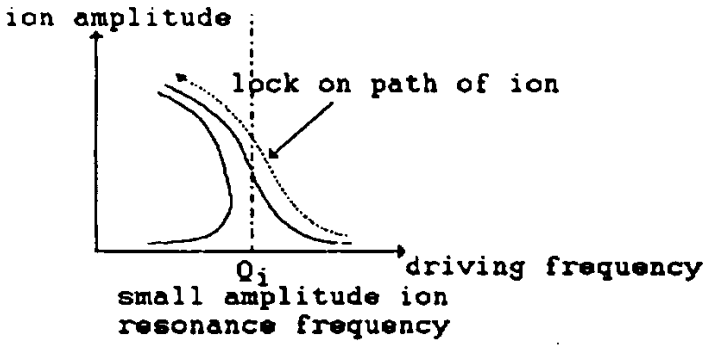

Fig. 16 Qualitative Amplitude response curve of an ion versus the driving frequency near resonance.

This asymmetry has been verified both in the CERN and Fermilab antiproton accumulators and in the EPA ring [102] [105]. Figure 17 for the Fermilab AA, shows that shaking below a "slow wave" excited by ions is more efficient than shaking above, since it suppresses the instability signal.

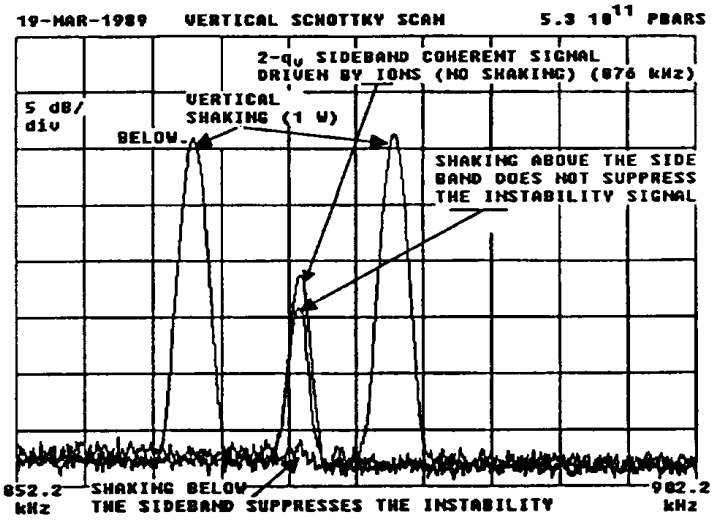

Fig. 17 Vertical Schottky scan showing the suppression of an ion-driven dipolar instability by shaking in the FNAL Antiproton Accumulator.

The analysis developed above simply hints at the reality. In fact, when one considers ions "locked" onto resonance, the amplitude of their coherent oscillation y_i depends only little on the amplitude of the excitation of the oscillating external force F in Eq. (44), when it is applied below or above a sideband [103]:

$$F \rightarrow F_{ef} = F \pm Q_i^2 \, \bar{y}_i, \qquad (x+n)^2 \gtrless Q^2 .$$

7. THE LIMIT OF ACCUMULATION

The containment of particles is in general due to the potential well. When charges start to accumulate, they diminish the depth of the potential well. The limit is reached when the density of accumulated charges is equal and opposite to the density of circulating charges so that the net resulting charge is null.

$$0 = d_i - d_p .$$

The neutralisation factor η is then, at most, equal to l. The beam is fully neutralised. Clearly the same limitation of neutralisation exists in bunched beams.

As we have seen, several clearing effects due to various drifts will limit the local neutralisation factor to less than 1. If required, clearing electrodes will collect electrons (or ions) and reduce the neutralisation in appropriate places. However, in some extreme cases the trapping of the ions or electrons is not due to the potential well, so that one could have local accumulation of charges to neutralisation levels higher than 1. We have seen that the undulators are probably very efficient in accumulating ions. Detailed calculations should be made in this particular case. It is not excluded that similar situations be found in the combination of end-fields of conventional magnets or quadrupoles.

8. THE EFFECTS OF NEUTRALISATION

There are several effects of neutralisation. The particles (ions or electrons) chased from the beam and hitting the wall with the energy of the potential well can create desorption. The ions stored in the beam modify the local pressure and therefore the life-time of stored beams. The most important effects come from the electric field of the ion (or electron) cloud. This induces a shift and a spread of

betatron oscillation frequencies and a coupling of horizontal and vertical motion. Finally, the ion cloud can interact as a whole with the beam and induce instabilities.

8.1 The pressure bump

The mechanism of the pressure bump is rather simple. In a beam of protons the ions are chased out of the potential well and hit the wall with enough energy to induce desorption of η molecules per ion (here η is the desorption factor and not the neutralisation factor). If the rate of filling the vacuum vessel with these molecules is higher than the pumping speed, the pressure will increase. The exact treatment is given in Refs. [62, 65]. It is however possible to obtain a first indication and order of magnitude by equating the pumping speeds to the desorption rate.

The equation of pumping of a vacuum vessel is in the absence of desorption [2]:

$$\frac{dP}{dt} = -\frac{SP}{V}$$

where P is the pressure (torr), S the pumping speed ($m^3 . s^{-1}$) and V is the volume (m^3) . In terms of molecular density d_m and linear pumping speed s, this can be written as

$$\frac{d}{dt} d_m = -\frac{s}{A} d_m \tag{46}$$

where A is the cross-sectional area of the vessel (and not a molecular mass).

The rate of production of ions *is* $(I/e)d_m\sigma$ ions per second and per metre *(I/e* is the number of protons per second and $d_m\sigma$ is the probability of ion production per metre). The desorption rate is therefore

$$\frac{d}{dt} d_m = \eta \cdot \frac{1}{A} \cdot \frac{I}{e} d_m \sigma . \tag{47}$$

Combining the two effects gives

$$\frac{d}{dt} d_m = \frac{d_m}{A}\left(\eta I \frac{\sigma}{e} - s \right) \tag{48}$$

leading to an exponential increase of density or pressure if

$$\eta I \frac{\sigma}{e} > s \ . \tag{49}$$

Ex: the ISR pressure bump at the beginning of operation

$$\eta = 4$$
$$I = 4$$
$$\frac{\sigma}{e} = 6.25 \times 10^{-4}$$

gives

$$\eta I (\sigma / e) = 10^{-2} \ \mathrm{m}^2 \cdot \mathrm{s}^{-1} .$$

If in some places the effective local pumping speed is reduced below 10 l s^{-1} m^{-1} the pressure bump can develop.

- The rise time of the pressure is of the order of A/s which is, for standard vacuum chambers, a few seconds. This could explain the oscillation of the vacuum pressure observed in a slow cycling machine with high currents like the PS or the Fermilab Main Injector.

- The desorption coefficient η depends on the energy of the ion striking the wall and therefore on the potential well depth: V_o. It also depends on the cleanliness of the vacuum chamber.

8.2 Pressure increase due to ions

The residual gas density and composition enter in the calculations of beam lifetime due to scattering of particles of the beam by the residual gas or of beam emittance growth due to multiple scattering.

The effective density to be considered is the sum of molecular and ionic densities.

We have seen (Eqs. 3 and 10) that the circulating beam density is

$$d_e = \frac{I}{e}\frac{1}{\beta c}\frac{1}{\pi a^2} \ . \tag{50}$$

The neutralisation factor η gives the ion density

$$d_i = \eta d_e .$$

The molecular density is

$$d_m = 3.3 \times 10^{22} P_m .$$

If we use the data of our nominal beam

$$d_e = 2.7 \times 10^{15}\ \mathrm{m}^{-3}$$

With 10% neutralisation

$$d_i = 2.7 \times 10^{14}\ \mathrm{m}^{-3}$$

corresponding to a 'partial pressure' :

$$P_i = 8 \times 10^{-9}\ \mathrm{torr}.$$

In ultra-high vacuum systems, the pressure increase due to ions can be equal to the residual gas pressure [43, 67, 72]:

8.3 Tune shifts

The problem of tune shifts induced by neutralisation is similar to the problem of tune shifts induced by space charge. One assumes that the transverse distributions of ions are the same as the distributions of circulating particles[6] .The calculations are made with constant real space density [7] for a beam of width *2a* and height *2b*. The ion density is *(*η is the neutralisation factor)

$$d_i = \frac{1}{2\pi R}\,\frac{1}{\pi a b}\,\eta\, n_e \ . \tag{51}$$

The electric field of this distribution has been calculated by several authors [7]; it can be written for the horizontal plane as (mks units)

$$\frac{\partial \varepsilon}{\partial x} = \frac{e}{\varepsilon_0}\frac{d_i}{1+\frac{a}{b}} \ . \tag{52}$$

The local quadrupole strength as defined in [1] is

---

[6] This assumption is made for the sake of simplicity. In fact , calculations [19] based on a one-dimensional linear model of the ion cloud motion show that this is not true. In that model, the width of the ion distribution is much smaller than the width of the electron beam distribution.

$$k = \frac{e}{E}\frac{\partial \varepsilon}{\partial x} \tag{53}$$

where E is the energy of the circulating particle.

The corresponding tune shifts are obtained using

$$\Delta Q = \frac{1}{4\pi}\int \beta(s)\, k(s)\, ds \ .$$

The tradition is to introduce the classical electron (or proton) radius

$$r_e = \frac{1}{E_0}\frac{e^2}{4\pi\,\varepsilon_0}, \tag{54}$$

where E_O is the rest mass of the electron. The integration is made around the circumference of the machine where β, a, b vary as a function of s. One usually replaces the quantities by their average around the machine ($\beta = R/Q$). This averaging is partly justified by the fact that the quantity $\pi a^2/\beta$ is an emittance.

$$\Delta Q_x = r_e \frac{1}{\gamma}\frac{R}{Q_x}\frac{1}{\pi a(a+b)}\eta \cdot n_e \tag{55}$$

$$\Delta Q_y = r_e \frac{1}{\gamma}\frac{R}{Q_y}\frac{1}{\pi b(a+b)}\eta \cdot n_e \ . \tag{56}$$

The values ΔQ_x, and ΔQ_y are in fact tune spreads as well as tune shifts because the distribution of ions is not uniform in the beam, so that the fields are strongly non-linear. The non-linearities of the field produced by the ion cloud introduce coupling effects[7]. This is particularly visible in e^+e^- machines [8, 12, 78]. These effects have been directly measured [66, 69].

8.4 Instabilities in proton beams

The motion of the electrons (or ions) in the potential well of the circulating beam and of the motion of the circulating beam in the electron cloud provides a feedback mechanism which can drive beam instabilities. Two such instabilities have been detected in proton machines. They received the name of ionic oscillations [110] and of electron instabilities [113]. The detailed theory of these instabilities does not have its place here. The mechanisms however are rather simple, and simplified formulae can be derived to obtain orders of magnitude.

8.4.1 The ionic oscillations

The proton bunches leave ion-electron pairs after their passage. With a bunched beam the light weight electrons are so stirred up in the ionisation process that they are lost to the wall almost immediately.

The heavy positive ions, even though they are of the same polarity as the beam, will stay longer in the vacuum chamber because they are created with thermal energies and are more difficult to move [110].

The detailed calculations go through the following steps:

---

[7] Recent calculations [18] show that the coupling produced by an ion cloud whose transverse distribution is a replica of the distribution of a symmetrical bi-gaussian flat beam is much smaller than what is observed experimentally [89]. This suggests that, either asymmetric ion distributions are present, creating stronger *linear* coupling or that other (possibly coherent) effects play a role in the phenomenon.

- a closed pattern of oscillation of the beam around the machine is defined:

$$x(\theta,t) = a\cos(Q-n)\Omega t + n\theta$$

which implies that at a given time (e.g. $t = 0$) the centre of gravity of the beam is distributed along n oscillations around the machine and that a given particle $(\theta = \theta_0 + \Omega t)$ oscillates with the betatron frequency $Q\Omega$. For simplicity we define

$$\omega = (Q - n)\Omega$$

then

$$x = a\cos(\omega t + n\theta) \tag{57}$$

- The corresponding pattern of ions will have the same aspect but with a phase shift due to the ion motion in the beam field.

$$x_i = b_0\cos(\omega t + n\theta) + b_1\sin(\omega t + n\theta)$$

We shall skip the difficult calculation of b_o and b_1.

- The presence of these ions will induce a force on the proton beam to be inserted in the equation of motion of the proton.

$$\ddot{x} + (Q\Omega)^2 x = K\cdot x_i \tag{58}$$

- The definition of x (Eq. (52)) no longer satisfies this equation of motion. The technique is to let the two constants a and ω vary slightly to take into account the small extra force introduced.

$$a \to a + \dot{a}t$$
$$\omega \to \omega + \partial\omega\ .$$

Then

$$\ddot{x} \cong -a(\omega + \partial\omega)^2\cos(\omega t + n\theta) - \dot{a}\omega\sin(\omega t + h\theta) \tag{59}$$

can be introduced in Eq. (58).

- The resolution of the cosine terms gives a negligible change in the tune shift. The resolution of the sine terms leads to the rate of rise of the instability.

$$\frac{1}{\tau_r} = \frac{\dot{a}}{a}$$

where τ_i is given as a function of b_0 and b_1.

- For $\tau_r > 0$ the amplitude is unstable. This is only obtained for $Q - n$ negative which means that only patterns with $n > Q$ will be unstable. This is a good signature of the instability.
- The final result [110] is remarkably simple for the dense beams which are common in present accelerators

$$\tau_r = \frac{8Q\gamma}{(n-Q)A}\tau_i$$

where τ_i is the ionisation time and A the atomic mass number of the ion.

For example at low energy ($\gamma \sim 1$) in the CERN PS ($Q = 6.25$, $n = 7$) with a pressure of 10^{-7} torr of N_2 ($A = 28$) one finds

τ_i = 10 ms τ_r = 20 ms

8.4.2 Electron-proton instabilities

This instability was first observed in the ISR. The field of the electrons accumulated in a proton beam induces a tune shift ΔQ. This effect can be introduced in the equation of motion of the protons [70, 113] (we have selected the vertical motion)

$$\ddot{z}_p + Q^2 \Omega^2 z_p = Q_p^2 \Omega \left(z_e - z_p \right) \tag{60}$$

where z_p and z_e are the transverse positions of the centre of gravity of the beam and of the electron cloud and Q_p is given by (Section 8.3)

$$Q_p^2 = 2Q\Delta Q = \frac{2r_p}{\gamma} \cdot R \cdot \frac{1}{\pi b(a+b)} \cdot n_e \,. \tag{61}$$

In a similar way the equation of motion of the centre of gravity of the electron cloud can be written as

$$\ddot{z}_p = Q_e^2 \Omega^2 \left(z_p - z_e \right) \tag{62}$$

with

$$Q_e = \frac{2}{\pi} \frac{r_e R n_p}{a(a+b)}.$$

As in the previous case we can define a pattern of oscillation of the proton beam

$$z_p = A_p \, e^{i(n\theta - \omega t)} \,. \tag{63}$$

Note that the introduction of the complex exponential will simplify the calculation of the phase shift and of the rate of rise that was treated with real sine and cosine functions in the previous example.

The electrons have only a local oscillation:

$$z_e = A_e \, e^{i\omega t} \,. \tag{64}$$

The substitution of Eqs. (58) and (59) in (55) and (57) gives two homogeneous equations in A_e and A_p. A_e and A_p can be eliminated with the result that the defined quantities must satisfy the resulting equation where the reduced frequency $x = (\omega/\Omega)$ has been introduced:

$$\left(Q_e^2 - x^2\right)\left[Q^2 + Q_p^2 - (n-x)^2\right] = Q_e^2 Q_p^2 \,. \tag{65}$$

In this equation Q_e , Q_p , Q and n are the parameters and x is the unknown.

If x is real it means that there exists a real frequency of oscillation of the system of two beams. The system is stable. If x is complex the solutions come by pairs; one with a positive imaginary part corresponding to a damping of the pattern; one with a negative imaginary part corresponding to an anti-damping of the pattern. A detailed examination of Eq. (65) shows that for large values of Q_p the solutions become complex.

The threshold value of Q_p is

$$Q_p^{th} = \frac{(n-Q_e)^2 - Q^2}{2\sqrt{Q_e(n-Q_e)}} \tag{66}$$

and defines the threshold of the instability. Above this threshold the imaginary part of the complex conjugate solutions x is

$$\mathrm{Im}\,\frac{\omega}{\Omega} = \frac{Q_p}{2}\sqrt{\frac{Q_e}{(n - Q_e)}}. \tag{67}$$

The growth is

$$\frac{1}{\tau_r} = \Omega\ \mathrm{Im}\,\frac{\omega}{\Omega}. \tag{68}$$

with $N_p = 6 \times 10^{13}$, $a = 3 \times 10^{-2}$ m, $b = 10^{-2}$ m, $\gamma = 16$ and $Q = 8.75$.

Then

$$Q_e = 200 \ \text{(Eq. (62))}.$$

The most dangerous mode n will give the smaller threshold Q_p^{th} This is obtained for n = 209 (Eq. (66))

$$Q_p^{th} = 0.052.$$

Equation (56) gives the corresponding average neutralisation required

$$\eta = \frac{n_e}{n_p} = 2 \times 10^{-3}$$

and Eqs. (67) and (68) give the growth rate

$$\tau_r = 8T$$

where T is the revolution period of the ISR

$$\tau_r = 25\ \mu\mathrm{s}.$$

The instability is extremely fast and the frequency observed is, in general, above the bandwidth of pick-up electrodes

$$\frac{1}{2\pi} Q_e\ \Omega = 64\ \mathrm{MHz}$$

8.4.3 Landau damping

In reality these instabilities are much less predictable than in the above simplified picture. The complexity comes when, instead of analysing the behaviour of the beam or of the ion cloud as a whole, one analyses the behaviour of each individual particle or ion before averaging the displacements. The fact that neutralisation forces are very non-linear, that the frequency of oscillation of electrons depends on the azimuth as well as the number of electrons trapped complicates the picture further. The calculations cannot be made on a single frequency but rather on a distribution of frequencies. It is far easier to explain why a given instability occurs in a given machine than why it does not occur in another machine.

8.5 Instabilities in antiproton beams

8.5.1 Coherent instabilities

Transverse coherent instabilities where collective oscillations of the beam centre or the beam shape grow exponentially due to the interaction with trapped ions have been identified in antiproton accumulators (coasting beams with negative space charge) at CERN and FNAL. These "two-beam" instabilities have been severe intensity limiting mechanisms for these machines, where they have been studied in detail [111].

For dipole instabilities, the theory outlined in Section 8.4.2 applies. The essential difference with proton machines trapping electrons is that the ionic oscillation frequencies in the beam potential well are much lower than with electrons (typically 1 to 2 MHz for H^+ and H_2^+, versus 20 to 80 MHz for electrons). The lowest transverse beam modes $(n - Q)\Omega$ are thus excited. These low frequency modes are the most unstable because of their low frequency spreads, resulting in loss of Landau damping.

For this reason, dipole instabilities driven by ions (H^+, H_2^+) occur at very low neutralisation levels (< 0.01), lower than in proton beams. The neutralisation resulting from a single neutralisation pocket around the ring created for instance by a localised vacuum chamber enlargement, may be sufficient to drive an instability [116]. Dipole instabilities can be effectively damped by a transverse feedback system using a high sensitivity resonant pick-up tuned at the frequency of the single unstable mode [108].

Quadrupole instabilities caused by ions, whereby the beam transverse shape or envelope oscillates, have also been identified in the CERN AA. This instability manifests itself as a kind of 'breathing' mode or fast emittance blow-up phenomenon causing eventually beam loss at a quadrupolar frequency $(n - 2Q)\Omega$ which can be as low as 400 kHz in the CERN AA.

The theory for this instability, similar to the dipolar one, is also well developed [117]. The threshold neutralisation at which this instability occurs is higher than the one for a dipole instability by a factor 2 to 4 depending on the type of quadrupole instability, for which four breathing modes exist. The required frequency spreads in ionic oscillations and beam mode frequencies for Landau damping to be effective are also lower by the same factors. In the CERN AA this instability appeared only after the dipole modes had been cured by transverse feedback damping.

8.6 Incoherent effects

These are single-particle phenomena, by comparison to coherent effects where the beam oscillates as a whole.

Tune shifts due to the space charge field created by trapped ions cause particles to cross resonance lines in the tune diagram:

$$nQ_x + mQ_y = \text{integer} \tag{69}$$

$$n, m = 0, \pm 1, \pm 2. \tag{70}$$

Very similarly to the excitation of non-linear resonances by the beam-beam interaction in colliding beam machines, the electrostatic field of ion clouds in neutralisation pockets causes non-linear detuning, and its uneven distribution may excite very high order resonances (up to 15th order in the CERN AA) [109]. This effect, still present at low neutralisation levels of a fraction of a percent, is very detrimental to antiproton accumulators which have low transverse emittance cooling rates.

8.7 Instabilities in electron beams

In electron storage rings that trap ions, the emission of synchrotron radiation by the circulating particles results in high damping rates of their transverse motion. It is unlikely that high order resonances can be harmful, since their strength decreases as their order increases. Otherwise, the physics of ion-beam interactions is similar to antiproton accumulators or proton machines. Coupling resonances excited by ions yield spectacular emittance effects, in particular in the vertical plane, where normally the beam size is naturally very small [78].

Transverse coherent instabilities may induce pulsations of the beam size. This occurs when the emittance growth rate due to an ion-induced instability is larger, and the neutralisation rate smaller than the natural damping rate. As the beam inflates ions are chased away by the instability, the beam then shrinks, neutralisation builds up again and the process repeats itself in a sort of relaxation mechanism [13].

Experience on modern machines shows that ion-induced tune shifts of a few 10^{-3} caused by neutralisation levels of a few percent or less, already present annoying emittance effects.

9. DIAGNOSTICS AND PHENOMENOLOGY

As described in the preceding sections, the presence of trapped species in a beam is diagnosed qualitatively by observation of the beam behaviour: intensity limitations, reduced particle lifetime, emittance blow up, coupling and coherent beam instabilities. To assess semi-quantitatively an effective degree of neutralisation is very difficult. The experimenter has essentially three possible means at his disposal, namely tune-shift measurements, ion clearing-current recordings and Bremsstrahlung diagnostics. None of these means is always applicable or absolutely rigorous. Nevertheless they can be powerful tools in understanding the rich phenomenology of ion-trapping physics.

9.1 Tune-shift measurements

The incoherent space-charge tune shift expressions (Eqs. (55), (56)) provide, in principle, a means to measure the average neutralisation in a beam. This supposes the possibility of clearing the beam of its ions (clearing electrodes, beam shaking, asymmetric bunch filling) so that from measurements of the tunes Q_x, Q_y with and without ions, the neutralisation η can be obtained from Eqs. ((50), (51)). $\Delta Q_{x,y}$ are usually extracted from frequency spectral analysis of a transverse betatron sideband (the difference signal from a pair of electrodes around a mode frequency $((n \pm Q)\Omega)$. Since the tune shift produced by ions is in this case incoherent, care must be taken to measure the incoherent tune (Schottky noise). This is an easy matter for unbunched beams like antiprotons. For electron beams, transverse coupled-bunch mode signals are more difficult to interpret precisely, particularly in cases of high neutralisation levels. Obtaining the maximum frequency shift experienced by a particle by comparison of two transverse spectra is only approximate; it pre-supposes the precise knowledge of the transverse distributions of the beam particles and of the ions. For ions, this distribution may vary from place to place around the ring and it cannot be measured. The measurement shown on Fig. 18, taken from the CERN AA, requires unfolding several spectra of the betatron oscillation amplitudes and the energy distributions of the beam particles [77]. If one supposes identical initial bi-gaussian transverse distributions for the beam particles and ions, the maximum frequency shifts $\Delta Q_{x,y}$ can be obtained by multiplying the shift of the peaks of the distributions by approximately 2.5 [87].

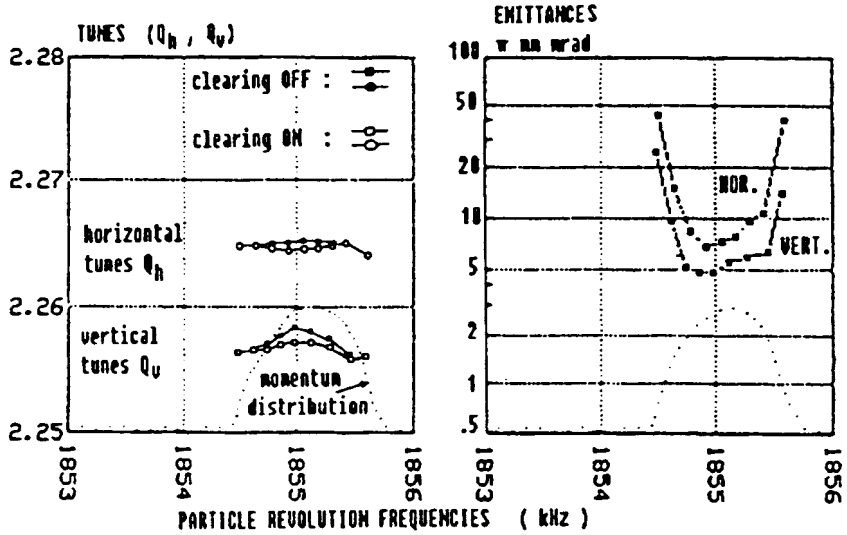

Fig. l8 Left: antiproton transverse tunes in the AA as a function of their momentum, with full (clearing off) and little (clearing on) neutralisation. Right: particle emittances. The tune shift with clearing off is consistent with an average neutralisation close to unity.

9.2 Clearing-current recordings

If ion clearing is procured by electrodes, and if secondary emission phenomena and direct photo-emission of electrons from these electrodes can be neglected (a serious difficulty for electron storage rings), the current drawn by electrodes is a direct measurement of the ion charge produced by

the beam. Electrodes are usually spread more or less evenly around a ring, with interspacing distances ranging from a few decimetres to several meters. Stable ions produced outside the field of action of electrodes are channelled by the beam to the nearest electrode, provided no potential barrier exists (magnet fringe fields, electrostatically charged insulators, etc.). On the other hand, unstable ions which are for instance destabilised by the bunching of the beam or shaken out of the beam potential by beam shaking, either voluntarily applied or resulting from ion-driven instabilities, do not end up on electrodes. Their absence, diagnosed as a temporary deficit on the recorded clearing current, provides a powerful means to understand the neutralisation phenomenology. The CERN AA for instance, equipped with a sophisticated ion clearing current monitoring system, has produced many interesting experimental results [88]. In machines with synchrotron radiation, clearing current measurements are rendered difficult — if not impossible - by the photo-emission of electrons produced by impinging photons on electrodes. On the CERN EPA however, a clearing electrode equipped with a shielding mask against synchrotron radiation and located at the end of a long straight section, has yielded some interesting measurements of the relative neutralisation levels for various bunch distributions (see Fig. 19), thus confirming theoretical predictions qualitatively [89].

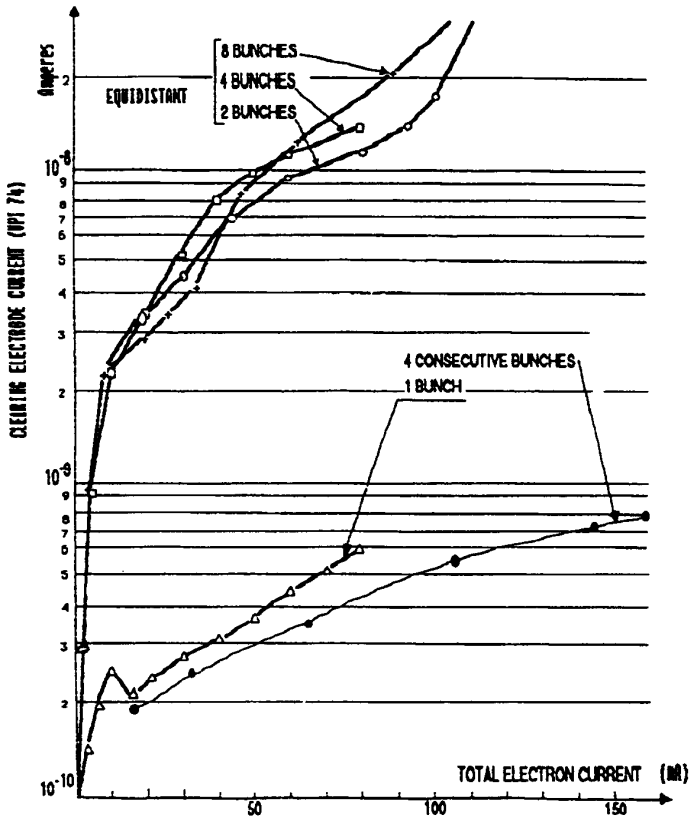

Fig. 19 Clearing current in the CERN electron accumulator for various bunch distributions. The less the neutralisation, the less the clearing current.

9.3 Bremsstrahlung measurements

High energy photons (gamma rays) are produced when the electrons of a circulating beam collide with the nuclei of ions trapped in the beam. By counting the number of these *bremsstrahlung* photons produced per second, one can estimate the density of target ions along the beam path seen by the detection system. This is a Cerenkov (lead-glass) or scintillator counter of dimensions large enough to contain the electromagnetic shower produced by the gammas. The whole system is aligned with the beam, looking through a metallic window in a bending magnet vacuum chamber at a straight section or a section of the beam orbit inside the dipole magnet.

The bremsstrahlung radiation covers a wide spectrum with energies extending up to the kinetic energy of the primary electron and has a very sharp collimation with a characteristic opening angle given by $1/\gamma$ where γ is the relativistic energy of the stored beam in units of the rest energy. This allows the use of lead collimation to prevent gamma rays from other sources (mainly shower debris from lost beam electrons) from reaching the detector.

An important advantage of this technique with respect to the more conventional tune shift measurements described above is that it allows the measurement of the local neutralisation rather than the average over the whole machine. However, since many different ion species may be trapped, some assumption must be made concerning the trapped-ion composition. In fact, since the total bremsstrahlung yield is proportional to the square of the atomic number of the target atom, the count rates are proportional to a weighted average of the ion densities, each ion species contributing with a weight Z^2. Also, collisions with the neutral residual gas molecules produce an additional bremsstrahlung yield which one must either evaluate theoretically from the known residual gas composition or experimentally, e.g., by running the machine with positrons or comparing different machine conditions (e.g. clearing electrodes on/off).

The first observations [90] were made in the KEK Photon Factory storage ring in the form of a correlation between sudden changes in lifetime with bursts of bremsstrahlung events. Later [91], bremsstrahlung count rates were registered in synchronism with a vertical blow-up caused by the accumulation of ions. The count rates as a function of time showed a rapid decrease at the time of the blow-up, followed by a slow increase which was attributed to the creation of new ions. The time constant for this slow rise was found to be in good agreement with the expected ionisation time for CO.

In Refs. [92, 93], a vertical blow-up was artificially produced by means of an external resonant excitation and the variation of the bremsstrahlung count rates was observed in both a uniform filling and partial filling modes of operation. Since the bremsstrahlung yield from the neutral residual gas molecules is expected to be independent of the beam dimensions, a decrease in the count rates during the blow-up was interpreted as a sign of the presence of trapped ions, and the comparison between the uniform filling and the partial filling confirms the theoretical prediction that fewer ions are present in the partial filling.

In Ref. [94], a study of the longitudinal motion of trapped ions is presented. Several gamma-ray counters were aimed at successive straight sections of the UVSOR storage ring. By looking at the time response of the count rates in these counters to a pulsed high voltage applied to a clearing electrode, the authors arrive at a spread in longitudinal ion velocities substantially larger than that expected from thermal considerations only.

REFERENCES

A considerable number of papers on the subject of neutralisation has been published. An attempt has been made to classify the large number of useful references.

[1] Y. Baconnier, A. Poncet, P.F. Tavares, "Neutralisation of Accelerator Beams by Ionisation of the Residual Gas", CERN 94-01, 1994.

[2] E.D. Courant and H. Snyder, "Theory of the alternating gradient synchrotron", Ann. Phys. (N.Y.) vol. 3, p. 1 (1958).

[3] J.D. Jackson, "Classical electrodynamics", John Wiley & Sons, New York, 1962.

[4] B. Rossi, "High energy particles", Prentice-Hall, Inc., Englewood Cligs, N.J., U.S.A., 1956.

[5] L. Spitzer, Jr., "Physics of fully ionized gases", Interscience Publishers, Inc., New York,1956.

REVIEWS, EARLY PAPERS

[6] B. Angerth, "Review of studies on beam neutralization in storage rings", CERN AR/Int.SG/65-1 (1965).

[7] R. Jolivot, "Anneaux de Stockage. Le piegeage des ions dans ACO et leur balayage", Rapport technique 75-63/RJ- FB, Ecole Normale Superieure - Faculte des Sciences, Orsay, Laboratoire de I'Accelerateur Lineaire (1963).

[8] R.D. Kohaupt, Ion clearing mechanism in the electron-positron storage ring DORIS" , DESY Ml-71/2 (1971).

[9] R. Alves Pires, J. Marriner, W. Marsh, A. Poncet, J. Rosensweig, and P. Zhou, Fermilab III Instabilities Workshop, Saint Charles, Illinois (1990).

[10] A. Poncet, "Ion trapping and clearing", CERN/MT 90-1 (ES). Course given at the the CAS, Uppsala, Sweden (October 1989) CERN 90-04 (1990).

[11] A. Poncet, "Ions and neutralization", CERN/MT 91-01. Talk given at the joint CERN/US particle accelerator school, Hilton Head Island, South Carolina, USA (November 1990) Springer Verlag, Lecture notes in Physics, n.400 (1992).

[12] D. Poteaux, "Piegeage des ions dans un anneau e+e-", Rapport technique 29-69 DP/LN Laboratoire de I'Accelerateur Lineaire, Orsay (1969).

[13] E.M. Rowe, "Trapped ion effects and their treatment in electron storage rings.", American Vacuum Society Series 5, AIP conf. proceedings No.171, p.193, New York (1988).

TRAPPED ION DYNAMICS

[14] Y. Baconnier and G. Brianti, "The stability of ions in bunched beam machines", CERN/SPS/80-2 (1980).

[15] C. Bernardini , "Space-charge efects in electron- synchrotrons", Nuovo Cimento, Vol X, N.5, p.804 (1988).

[16] L. Evans and D.J. Warner, "Space-charge neutralisation of intense charged particle beams: some theoretical considerations", CERN MPS/LIN 71-2 (1971).

[17] E. Fischer, "Space charges in electron storage rings and the removal of positive ions by a D.C. clearing field", PS/Int. AR/60- 14 (1960).

[18] P.F. Tavares, "Betatron coupling in ion loaded electron beams", CERN PS/92-54 (LP) (1992).

[19] P.F. Tavares, "Transverse distribution of ions trapped in an electron beam", CERN PS/92-55 (LP) (1992).

PARTIAL FILLING, GAPS

[20] M. Barton,"Ion trapping with asymmetric bunch filling of the NSLS VUV ring", Nucl. Instrum. Methods, A243 p.278 (1986).

[21] D. Douglas, "Ion stability in bunched electron beams", IEEE Trans. Nucl. Sci. Vol. Ns-32, No.5 p.2294 (1985).

[22] S. Sakanaka, "The stability of ions in partially filled mode operation in the electron storage ring", KEK 86-17 (1986).

LONGITUDINAL MOTION

[23] Y. Miyahara, K. Takayama, and G. Horikoshi, "Dynamical analysis of the longitudinal motion of trapped ions in an electron storage ring", Nucl. Instrum. Methods, A270 p.217 (1988).

[24] D. Sagan, "Some aspects of the longitudinal motion of ions in electron storage rings", Nucl. Instrum. Methods, A307 p.171 (1991).

BEAM POTENTIAL CALCULATIONS AND MEASUREMENTS

[25] M. Bassetti and G.A. Erskine, "Closed expressions for the electrical field of a two dimensional Gaussian charge", CERN-ISR-TH/80-06 (1980).

[26] 0. Grobner and K. Hübner, "Computation of the electrostatic beam potential in vacuum chambers of rectangular cross-section", CERN/ISR-VA/75-27 (May 1975).

[27] M. Gygi-Hanney and B. Zotter, "Field strength in a bigaussian beam", LEP theory note 44 (1987).

[28] L.J. Laslett, “Potential of a uniformly charged beam with an elliptical cross-section”, ERAN-44 (November 1969).

[29] L.J. Laslett, "Image field of a straight beam of elliptical cross-section", ERAN-49 (1970).

[30] R. Alves-Pires, "Beam dimensions and beam potential in the CERN Antiproton Accumulator complex", CERN PS/87-70 AA (1987).

[31] R. Alves-Pires, "Conformal mapping for two-dimensional electrostatic beam potential calculations", CERN PS/87-66 (1987).

[32] E. Regenstreif, "Potential and field created by an elliptic beam inside an infinite cylindrical vacuum chamber of circular cross-section", CERN/PS/DL 77-37 (1977).

[33] E. Regenstreif, "Potential and field created by a rectangular beam inside an infinite cylindrical vacuum chamber of circular cross section", CERN PS/DL 77-31 (1977).

[34] P. Strubin, "ISR Performance Report-Run 750, 7 July 1976, 26 GeV-Measure of the beam potential as a function of beam current, ISR-VA- ISR-VA-PS/srn (24th August, 1976).

DUST TRAPPING

[35] P. Marin, "Microlosses of beam current in Super-ACO operated with electrons", Lure RT/90-01 (1990).

[36] P. Marin, "Longitudinal motion of a dust particle along a beam of electrons in a storage ring", Lure RT/90-06 (1990).

[37] P. Marin, "Observation of bremsstrahlung on dust particles trapped in electron beams at DCI and Super-AM, Lure RT/91-03 (1991).

[38] F. Pedersen, "Effects of highly charged, solid macroparticles in negatively charged circulating beams", CERN PS/87-25 (1987).

[39] H. Saeki, T. Momose, and H. Ishimaru, "Observations of dust trapping phenomena in the Tristan accumulation ring and a study of dust removal in a beam chamber", Rev.Sci.Instrum. Vol.62 No.4 p.874 (1991).

[40] D. Sagan, "Mass and charge measurement of trapped dust in the CESR storage rings", Cornell BN 92-12 (1992).

[41] C.J. Bochetta and A. Wrulich, "The trapping and clearing of ions in ELETTRA", Sincrotrone Trieste ST/M-88/26 (1988).

[42] E. Bozoki and H. Halama, "Ion related problems for the XLS ring", Nucl. Instrum. Methods, A307 p.156 (1991) .

[43] G. Brianti, "Upper limits of the average luminosity in the SPS p-p collider", CERN/SPS/DI/80-1 (20th February, 1980).

[44] F. Caspers, J.P. Delahaye, J.C. Godot, K. Hubner, and A. Poncet, " EPA beam-vacuum interaction and ion-clearing system", EPAC p. 1324, Rome (1988).

[45] S. Chattopadhyay, "Coherent instability and ion trapping considerations for Alladin lattices", LBL-19281 (1985).

[46] R.C. Gluckstern and A.G. Ruggiero, "Ion production and trapping in electron rings", BNL-26585 (1979).

[47] J. Herrera and B. Zotter, "Average neutralisation and transverse stability in Isabelle", BNL 50980 UC-28 (1978).

[48] T. Kasuga, "Ion clearing system for the UVSOR storage ring", Jpn. J. Appl. Phys. Vol.2 No.11, p.1711 (1986).

[49] R.Z. Liu, "Considerations on ion accumulation and clearing in Spear". SSRL ACDNote 25 (1984).

[50] F. Pedersen, A. Poncet, and L. Soby. "The CERN Antiproton Accumulator clearing system with ion current as a residual neutralization diagnostic", CERN PS/89-17 ML (1989).

[51] A. Poncet, "Ion clearing in EPA", PS/ML/Note 83-1 (1983).

[52] A. Poncet, "Quel vide pour I'EPA?", PS/ML/Note 83-3 (1983).

[53] D. Sagan, "Ion trapping in the CESR B-Factory", Cornell, CBN 91-2, (May 1990).

[54] Y. Sun, "A preliminary report on ion clearing in Spear", SSRL ACD-note 83 (may 1990).

[55] P.F. Tavares, "The ion clearing system of the UVX-2 synchrotron radiation source", Proceedings 3rd EPAC, p.1647, Berlin (1992).

[56] E.J.N. Wilson, "Does ion trapping produce a large space charge •Q in the LEP injector chain?", CERN/SPS-DI LTD (1980).

[57] Workshop on pp in the SPS. (Theoretical aspects of machine design, March 1980), SPS-pp-1, 9th May, 1980.

[58] P. Zhou and J.B. Rosenzweig, "Ion trapping in Tevatron with separated orbits", Fermilab III Instabilities Workshop, Saint Charles, Illinois (1990).

NEUTRALISATION IN THE ISR

[59] B. Angerth, E. Fischer, and 0. Grobner, "The clearing fields of the ISR, CERN ISR-VA/71-47 (1971).

[60] R. Calder, E. Fischer, 0. Grobner, and E. Jones, "Vacuum conditions for proton storage rings", CERN/ISR-VA/74-26 (1974).

[61] E. Fischer, "Clearing fields for the ISR", ISR-VAC/66-15, (1966).

[62] E. Fischer and K. Zankel, "The stability of the residual gas density in the ISR in presence of high intensity proton beams". CERN-ISR-VA/ 73-52 (1973).

[63] 0. Grobner, "ISR Performance Report- Clearing studies using Langmuir probe technique Run 139, 22 GeV, 20 bunches", ISR-VA/OG/ss (1972).

[64] 0. Grobner, "ISR Performance Report- Run 142 , 26 GeV, 20 bunches, Ring 1, 26 FC, Beam Decay as Function of Clearing Voltage", ISR-VA/OG/ss, (1972).

[65] 0. Grobner and R.S. Calder, "Beam induced gas desorption in the CERN intersecting storage rings", IEEE Trans.Nucl.Sci. , Vol. NS-20, No 3 p.760 (1973).

[66] 0. Grobner, "ISR Performance Report- Attempt to measure neutralisation shifts", ISR-VA/OG/srn (1974).

[67] 0. Grobner and P. Strubin, "ISR Performance Report -Decay rate due to nuclear scattering pressure as determined from the clearing currents", ISR-VA/OG/sm, llth July, 1974.

[68] 0. Grobner, "ISR Performance Report- Clearing, Pressure Bump, Beam Behaviour", ISR-VA/OG/srn (1975).

[69] 0. Grobner, "Performance study on proton- proton storage rings at several hundred GeV/c. Neutralisation and vacuum requirements in ISR". CERN/ISR-AS/74-67 (1974).

[70] 0. Grobner, "ISR Performance Report - RF Clearing, e-p lines and electron noise", ISR-VA/OG/srn (1975).

[71] 0. Grobner, "An estimate of the rate of electron removal by RF-clearing". ISR VA/OG (1975).

[72] 0. Grobner, "ISR Performance Report- -Run 904, 26 GeV, 6.12.77. Observation of beam blow-up by multiple scattering on neutralising electrons", ISR-VA/OG/srn (1978).

[73] 0. Grobner, "Ion clearing of anti-proton beams in the ISR", CERN ISR-VA/OG/srn (1978).

[74] 0. Grobner, "ISR Performance Report-Run 389, Ring 1, Dependence of clearing current on neutralisation", ISR-VA/OG/srn (1984).

[75] Technical Note - ISR Vacuum Group, "The behaviour of ions in presence of a bunched antiproton beam in the ISR", ISR-VA/EF-sm, 7th November 1978.

[76] D.G. Koshkarev, "Concerning a new way of removing electrons from an unbunched electron beam", ISR-DI/DGK (1974).

[77] S. Van der Meer, "Measurement of transverse stack emittances from Schottky scans", PS/AA/Note 84-11 (1984).

NEUTRALISATION EXPERIMENTS

[78] M.F. Biagini et al., "Observation of ion trapping at Adone", llth Intemational conference on high energy accelerators,p. 687, Geneva (1980).

[79] E.V. Bulyak and V.I. Kurilko, "Low frequency transverse charge oscillations in an electron storage ring", JETP Letters Vol.34, No. 9 p.471 (1981).

[80] E.V. Bulyak and V.I. Kurilko, "Space charge neutralization of a beam in high current electron storage rings", Sov. Phys. Tech. Phys. Vol.27, No.2 p.194 (1982).

[81] T.S. Chou and H.J. Halama, "Trapped ions and beam lifetime in the NSLS storage rings", Proceedings of the EPAC, p.1773, Rome (1988).

[82] R. Cappi and J.P. Riunaud, "Trapped ion effects with electron beams in the CERN PS", CERN/PS 90-17 PA (1990).

[83] 0. Grobner, "ISR Performance Report- Measurement of the self-clearing rate as function of beam current, ISR- VA/OG/sm, 27th March, 1975.

[84] H. Halama and E. Bozoki, "Ion clearing and photoelectron production in the 200 MeV SXLS ring", BNL-46471 (1991).

[85] T. Kasuga, H. Yonehara, T. Kinoshita, and M. Hasumoto, "Ion trapping effect in the UVSOR storage ring", Jpn. J. Appl. Phys. Vol.24, No.g p.1212 (1985).

[86] P. Marin, "Positron versus electron behaviour in Super- ACO", Lure RT/Anneaux/90-03 (1990).

[87] W. Marsh, "How to measure beam neutralization in the accumulator", Fermilab III Instabilities Workshop, SaintCharles, Illinois (1990).

[88] F. Pedersen et al, "The CERN Antiproton Accumulator clearing system with ion current measurements as a residual neutralisation diagnostic", CERN PS/89-17 (ML) (1989).

[89] A. Poncet, 'Trapping of ions in the EPA electron beam. Stability conditions and diagnosis", CERN PS 88-14 ML (1988).

BREMSSTRAHLUNG EXPERIMENTS

[90] M. Kobayashi et al, "Observations of bremsstrahlung caused by ion trapping", Proceedings of the 5th Symposium of Accelerator Science and Technology, KEK (1984).

[91] H. Kobayakawa et al, "Observation of the ion trapping phenomenon with bremsstrahlung", Nucl. Instrum. Methods, A248 p. 565 (1986).

[92] S. Sakanaka et al, "Observation of ion trapping in single bunch operation at the Photon Factory storage ring", KEK 87-168 (1987).

[93] S. Sakanaka et al, "Differences in ion trapping between uniform and partial filling", Nucl. Instrum. Methods, A256 p.184 (1987).

[94] K. Watanabe et al., "Drift velocity and pulse response of trapped ions in a circulating electron beam", Jpn. J Appl. Phys., Vol.26, No.12 , L1964 (1987).

IONISATION, HEATING, COOLING

[95] U. Amaldi, "Fisica delle radiazioni", Boringhieri, Torino (1971).

[96] F. Lapique and F. Piuz, "Simulation of the measurement by primary cluster counting of the energy lost by a relativistic ionizing particle in argon", Nucl. Instrum. Methods, 175 p. 297 (1980).

[97] Y. Miyahaxa, "Photo-ionization of residual gas in electron storage ring", Jpn. J. Appl. Phys., Vol. 26, No. 9, p.1544

[98] F. Rieke and W. Prepjchal, "Ionisation cross-section of gaseous atoms and molecules for high-energy electrons and positrons" , Phys.Rev. A Vol. 6, No. 4 , p.1507 (1972).

[99] F. Sauli, "Principles of operation of multiwire proportional drift chambers", CERN 77-09 (1977).

[100] K. Symon, "Are clearing electrodes really necessary?", Private Comunication (1964).

BEAM SHAKING

[101] E. Bozoki, "Ion shaking in the 200 MeV XLS-ring". Proceedings 3rd EPAC, p.789, Berlin (1992).

[102] J. Marriner, D. Möhl, Y. Orlov, A. Poncet and S. Van der Meer, "Experiments and practice in beam shaking", CERN/PS/89-48 AR (1989).

[103] Y. Orlov, "The suppression of transverse instabilities caused by trapped ions in the AA by shaking the $\bar{p}$ beam", CERN/PS/89-01 (1989).

[104] R. Alves-Pires, "Beam shaking for the Fermilab Antiproton Accumulator", Femilab III Instabilities Workshop, Saint Charles, Illinois (1990).

[105] A. Poncet and Y. Orlov, "EPA machine experiment note - ion shaking tests", PS/ML/Note 89-1 (1989).

[106] J.B. Rosenzweig, "Beam-ion cyclotron resonance instability", Fermilab III Instabilities Workshop, Saint Charles, Illinois (1990).

[107] P. Zhou and J.B. Rosenzweig, "Ion clearing using Cyclotron shaking", Fermilab III Instabilities Workshop, Saint Charles, Illinois (1990).

INSTABILITIES

[108] G. Carron et al, "Observation of transverse quadrupole instabilities in intense cooled antiproton beams in the AA", CERN/PS/89-18 (AR), Proceedings PAC, p.803, Chicago (1989).

[109] A. Dainelli, "Antiproton-positive ion transverse instabilities in the CERN AA". A tune modulated direct map simulation", CERN/PS/87-13 (AA) (1987).

[110] H.G. Hereward, "The instability of radial betatron oscillations in the CPS", CERN MPS/Int. DL 64-8 (1964).

[111] E. Jones et. al, "Transverse instabilities due to beam trapped ions and charged matter in the CERN AA", IEEE Trans.Nucl.Sci., Vol. NS -32, p. 2218 (1985).

[112] Y. Kainiya, M. Yzawa, T. Katsura, and M. Kihara, "Vertical instability caused by ion trapping in KEK-Photon factory storage ring", Proc. of 5th Symp. Acc. Sci. Tech. p.148 (1984).

[113] E. Keil and B. Zotter, "Landau-damping of coupled electron-proton oscillations", CERN-ISR-TH/71-58 (1971).

[114] D.G. Koshkarev and P.R. Zenkevich, "Resonance of coupled transverse oscillations in two circular beams", Part. Acc. Vol.3 p.1 (1972).

[115] L.J. Laslett, A. Sessler, and D. Möhl, "Transverse two-stream instability in the presence of strong species-species and image forces", Nucl. Instrum. Methods, Vol. 121 p.517 (1974).

[116] F. Pedersen, and A. Poncet, "Proton-antiproton instability in the CERN AA", CERN PS/AA/ME Note 81, 1981

[117] R. Alves-Pires et. al, "On the theory of coherent instabilities due to coupling between a dense cooled beam and charged particles from the residual gas", CERN/PS/89-14 (AR), PAC p.800 Chicago (1989).

[118] R. Alves-Pires and D. Möhl, "Landau damping of coupled quadrupole modes", PS/AR/Note 90-09 (1990).

ANNEX I

COMPUTATION OF THE MEAN VELOCITY IN THERMAL MOTION

By integration from $-\infty$ to $+\infty$ of the Boltzman equation (Section 4.1) over υ_x and υ_y one obtains the equation

$$\frac{dn}{d\upsilon_x} = d_m \sqrt{\frac{m}{2\pi kT}} e^{-m\frac{\upsilon_x^2}{2kT}}.$$

The mean value of υ_x is by definition

$$\langle \upsilon_x \rangle = \frac{1}{d_m} \int_{-\infty}^{+\infty} \upsilon_x \frac{dn}{d\upsilon_x} d\upsilon_x = 0.$$

We are interested in the mean velocity in one direction. Either:

$$\langle |\upsilon_x| \rangle 0 \geq = \frac{1}{d_m/2} \int_0^{+\infty} \upsilon_x \frac{dn}{d\upsilon_x} d\upsilon_x$$

or

$$\langle |\upsilon_x| \rangle = \frac{1}{d_m} \int_{-\infty}^{+\infty} |\upsilon_x| \frac{dn}{d\upsilon_x} d\upsilon_x$$

In both cases the result is

$$\langle |\upsilon_x| \rangle = \sqrt{\frac{2kT}{\pi \cdot m}}$$

and therefore $\langle |\upsilon_x| \rangle = \upsilon_m / 2$ and not $\upsilon_m/4$ as quoted in several papers.

ANNEX II

ELLIPTICAL VACUUM CHAMBER AND BEAM

The detailed calculation of the potential in a rectangular vacuum chamber of width 2*w* and height 2*h* induced by a beam with current *I*, velocity βc, height *2b* and width *2a* has been made [26]. The following formulae allow the detailed computation of the potential at the centre of the beam:

$$U_0 = \frac{I}{\beta c\, \varepsilon_0}$$

$$\eta_s = \frac{\pi}{2w} s$$

$$C_s = \frac{U_0}{4bw} \frac{g_s}{\eta_s}$$

$$g_s = \frac{\cos \eta_s (\omega - a) - \cos \eta_s (w + a)}{\eta_s \cdot a \left(1 - n_s^2 \frac{a^2}{\pi^2}\right)}$$

Then the potential in the centre is

$$V(0,0) = \sum_s \left(1 - \frac{\cos h\left[n_s (h-b)\right]}{\cos h\, \eta_s \cdot h}\right) C_s \sin \eta_s\, w \cdot$$

ANNEX III

NUMERICAL VALUE (MKS UNITS)

ε	=	8.85×10^{-12}	($F \cdot m^{-1}$ or $C\ v^{-1}\ m^{-1}$)
μ_0	=	$4\pi \times 10^{-7}$	($H \cdot m^{-1}$ or $A^{-1}\ V\ s \cdot m^{-1}$)
C	=	3×10^{8}	($m\ s^{-1}$)
r_p	=	1.53×10^{-18}	(m)
r_e	=	2.82×10^{-15}	(m)
m_p	=	1.67×10^{-27}	(kg)
m_e	=	9.10×10^{-31}	(kg)
m_p/e	=	1.0×10^{-8}	($T \cdot s$ or $kg\ C^{-1}$)
m_e/e	=	5.7×10^{-23}	($T \cdot s$ or $kg\ C^{-1}$)
h	=	6.85×10^{-16}	$eV \cdot s$
k	=	1.4×10^{-21}	J